horticulturae

MDPI

Article

Intracellular Water Dynamics Are Associated with Contrasting Drought Responses in *Broussonetia papyrifera* (L.) Vent. and *Morus alba* L.

Liang Luo [1,2] and Yanyou Wu [2,*]

[1] College of Science, Kaili University, Kaili 556011, China; luoliang0911@163.com
[2] State Key Laboratory of Environmental Geochemistry, Institute of Geochemistry, Chinese Academy of Sciences, Guiyang 550081, China
* Correspondence: wuyanyou@mail.gyig.ac.cn

Abstract

Drought severely constrains plant growth and physiological functions, particularly in karst ecosystems where shallow and heterogeneous soils further exacerbate water limitations. However, changes in intracellular water dynamics during progressive drought and their relationship with photosynthetic responses remain poorly understood. Here, we subjected seedlings of *Broussonetia papyrifera* (L.) Vent. and *Morus alba* L. to progressive drought for 16 days under two simulated habitat conditions: rock outcrop (RO) and non-rock outcrop (NRO). At nine progressive drought stages, we measured soil water content (SWC), leaf water potential (Ψ), net photosynthetic rate (P_n), stomatal conductance (gsw), transpiration rate (E), and four impedance-derived intracellular water parameters: intracellular water-holding capacity (IWHC), intracellular water transport rate (IWTR), intracellular water-holding time (IWHT), and intracellular water-use efficiency (IWUE). During progressive drought, SWC declined and Ψ became more negative. IWHC, IWTR, P_n, gsw, and E also declined, whereas IWHT generally increased; IWUE showed species-specific temporal patterns. *M. alba* L. exhibited earlier declines in Ψ, IWHC, IWTR, and photosynthetic traits, whereas *B. papyrifera* L. showed more gradual physiological changes and maintained comparatively higher water status. IWHC and IWTR were positively correlated with photosynthetic traits, whereas IWHT showed negative associations. These correlations suggest that intracellular water dynamics may complement conventional measurements for characterizing species-specific responses to drought. In particular, IWHT increased during drought and may reflect a temporal dimension of intracellular water regulation; however, causality and predictive capacity remain to be tested.

Keywords: karst ecosystem; electrical impedance; photosynthetic adjustment; leaf water potential; woody species

Check for updates

Received: 10 September 2026
Revised: 12 October 2026
Accepted: 28 October 2026
Published: 30 October 2026

Copyright: © 2026 by the authors. Licensee MDPI, Basel, Switzerland. This article is an open access article distributed under the terms and conditions of the Creative Commons Attribution (CC BY) license.

1. Introduction

Drought is a major environmental constraint on plant growth, productivity, and ecosystem functioning worldwide [1,2]. Climate change is intensifying water limitation for vegetation in many regions, highlighting the need to understand how plants maintain water status and carbon assimilation as drought progresses [3,4]. Plant responses to drought involve coordinated adjustments in water relations, stomatal regulation, photosynthesis, and water transport [5,6]. However, the timing and coordination of these responses may differ among

species, and this variation may influence their capacity to maintain physiological functions as water availability declines.

Karst environments are susceptible vulnerable to water limitation because extensive bedrock exposure, high bedrock permeability, and shallow, discontinuous soils constrain soil water storage and plant-available water [7,8]. The complex soil–rock structures characteristic of karst landscapes further create substantial spatial and temporal heterogeneity in water storage and availability, thereby influencing vegetation productivity and plant water uptake [9,10]. Plants growing in karst ecosystems can adjust their water sources and water-use strategies in response to variations in water availability, and seasonal shifts in water uptake are associated with changes in transpiration and water-use efficiency [11,12]. Moreover, recent studies indicate that plant water-use efficiency in karst ecosystems is influenced by the interaction of hydrological, climatic, and vegetation-related factors [13]. Consequently, understanding how plants coordinate water status and carbon assimilation under progressive drought is particularly important for assessing responses to drought in karst vegetation.

Leaf water potential (Ψ) is widely used to characterize plant water status, whereas gas-exchange parameters such as net photosynthetic rate (P_n), stomatal conductance (gsw), and transpiration rate (E) provide complementary information on photosynthetic responses under water limitation [14,15]. As drought progresses, declining soil water availability can reduce Ψ more negative and alter plant water supply, while stomatal closure and reductions in photosynthetic activity can constrain carbon assimilation [16,17]. However, conventional measurements of leaf water status and gas exchange provide limited information about the dynamics of water within leaf tissues. Recent studies based on physiological impedance measurements have introduced quantitative parameters describing intracellular water-holding capacity (IWHC), intracellular water transport rate (IWTR), intracellular water-holding time (IWHT), and intracellular water-use efficiency (IWUE), providing an additional perspective on intracellular water regulation [18,19]. These parameters may complement conventional measurements by describing changes in intracellular water properties during water limitation.

The coordination between intracellular water dynamics and photosynthetic performance may be particularly important during progressive drought, as plants experience progressively declining soil water availability and sequential physiological adjustments. Recent evidence suggests that intracellular water dynamics are closely linked to photosynthetic activity and plant growth under water limitation [20]. Moreover, woody plants exhibit substantial interspecific variation in hydraulic regulation, water-use strategies, and drought responses [21]. Similar variation occurs among woody species in karst ecosystems, where differences in rooting characteristics and water uptake strategies can influence plant responses to heterogeneous water availability [22]. Therefore, comparing species with contrasting ecological and physiological traits provides a useful framework to examine how intracellular water regulation is coordinated with plant water status and photosynthetic performance during progressive drought.

Broussonetia papyrifera (L.) Vent. and *Morus alba* L. are widely distributed woody species with contrasting ecological and utilization traits in karst regions. Previous studies have reported interspecific differences in photosynthetic characteristics, water-use responses, and physiological adjustments under water limitation [19,23]. These contrasting responses provide a suitable comparative framework for examining how woody plants coordinate intracellular water regulation and photosynthetic activity under progressive water limitation. Nevertheless, the temporal coordination among intracellular water dynamics, Ψ, and photosynthetic performance during progressive drought remains poorly understood.

The objectives of this study were to (1) quantify changes in intracellular water dynamics and photosynthetic traits during progressive drought in *B. papyrifera* L. and *M. alba* L.; (2) evaluate the relationships among intracellular water dynamics, plant water status, and photosynthetic performance; and (3) identify physiological traits most closely associated with species-specific responses to drought using multivariate analysis. We hypothesized that progressive drought would be accompanied by coordinated changes in intracellular water dynamics and photosynthetic performance, and that IWHT might provide complementary information for characterizing these responses. We further hypothesized that the two species would differ in the temporal coordination of intracellular water retention and transport during progressive drought.

2. Materials and Methods

2.1. Study Species and Experimental Design

This experiment was conducted under controlled greenhouse conditions with two woody plant species—*Broussonetia papyrifera* (L.) Vent. and *Morus alba* L.—and two simulated habitat conditions: rock outcrop (RO) and non-rock outcrop (NRO). The soil used for both treatments was collected from a calcareous soil derived from carbonate bedrock in Qingzhen City, Guizhou Province, China. The soil was air-dried and thoroughly mixed, and then an equal mass of soil was added to each pot. The two treatments differed in rock configuration: in the RO treatment, limestone fragments were placed at the bottom of each pot, with additional limestone fragments arranged along one side of the soil surface; the NRO treatment contained the same soil but without these limestone additions.

Four independent pots were established for each species-by-habitat combination, with four plants of the same species grown in each pot. Each pot served as the independent experimental unit. Measurements from the four plants within each pot were averaged to obtain one pot-level observation. Thus, each species-by-habitat combination had four replicate pots ($n = 4$), and measurements across the nine drought stages were treated as repeated measures on the same pots. The pot was included as a random effect in the statistical models.

2.2. Progressive Drought Treatment

Before drought initiation, all pots were thoroughly watered to establish comparable initial water conditions. Irrigation was then withheld for 16 days to impose progressive drought. Soil water content (SWC) gradually declined during the experimental period, creating a gradient of drought progression from D0 to D16.

Measurements were conducted at nine drought stages (D0, D2, D4, D6, D8, D10, D12, D14, and D16). At each stage, SWC, leaf water potential (Ψ), photosynthetic traits, and impedance-derived intracellular water parameters were measured. The same plants were monitored throughout the experiment, and no plants were replaced. Measurements were thus repeated on the same pots over time.

2.3. Soil Water Content (SWC) and Leaf Water Potential (Ψ)

Soil water content (SWC, %) was determined gravimetrically using soil samples collected from the 0–20 cm soil layer.

Leaf water potential (Ψ, MPa) was measured using a PSYPRO water potential system (Wescor, Inc., Logan, UT, USA) with a C-52 sample chamber. Small leaf discs were collected from fully expanded leaves using a hole punch and immediately placed into the C-52 sample chamber. Different leaves were used at each drought stage to avoid measuring damaged tissue, allowing the same pots to be repeatedly measured across all nine stages [23].

2.4. Photosynthetic Measurements

Net photosynthetic rate (P_n, μmol CO_2 m^{-2} s^{-1}), stomatal conductance (gsw, mol H_2O m^{-2} s^{-1}), and transpiration rate (E, mmol H_2O m^{-2} s^{-1}) were measured using a portable photosynthesis system (LI-6800, LI-COR Biosciences, Lincoln, NE, USA) under stable environmental conditions. Fully expanded mature leaves were selected for measurements, and standard gas-exchange procedures were followed [15].

Instantaneous water-use efficiency (WUE) was calculated as the ratio of P_n to E:

$$\mathrm{WUE} = \frac{P_n}{E} \quad (1)$$

where P_n and E denote the corresponding photosynthetic and transpiration rates, respectively.

2.5. Measurement of Intracellular Water Dynamics

Intracellular water dynamics were quantified using the physiological impedance method described by Xing et al. [18]. This approach characterizes the electrical impedance properties of leaf tissues using an equivalent electrical circuit representing extracellular, membrane, and intracellular components (Figure 1). The corresponding impedance parameters were used to characterize intracellular water-related physiological properties following the calculation procedures described by Xing et al. [18] and Yu et al. [19].

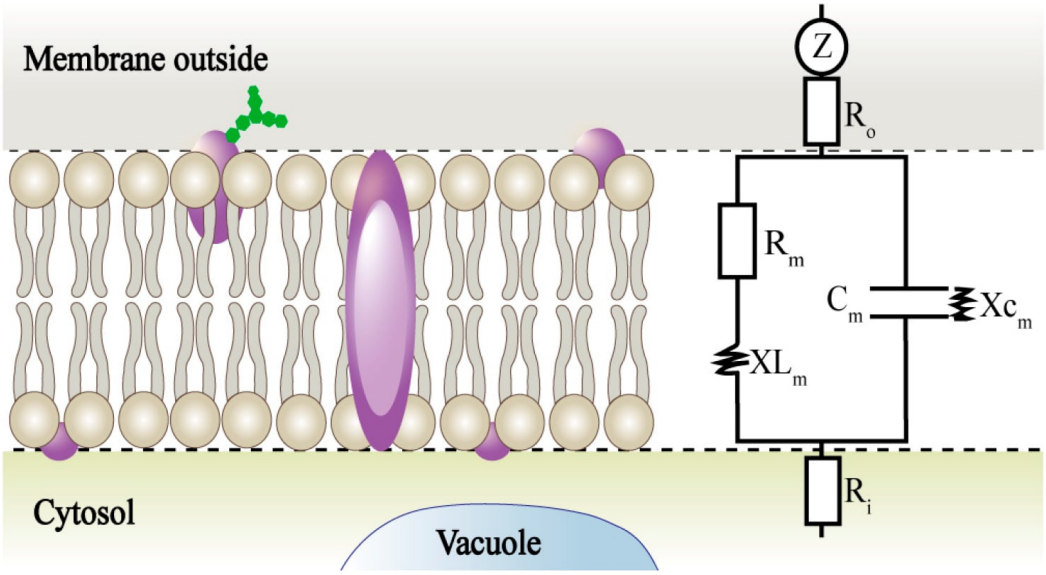


Figure 1. Schematic representation of the physiological impedance model used to characterize intracellular water dynamics in leaf tissues. The equivalent electrical circuit represents the electrical properties of extracellular, membrane, and intracellular components of the leaf tissue.

Four intracellular water-related parameters were evaluated: IWHC, IWTR, IWHT, and IWUE. IWHC was used to characterize the capacity of leaf tissues to retain intracellular water, whereas IWTR represented the rate of intracellular water transport. IWHT reflected the duration of intracellular water retention, and IWUE provided an indicator of intracellular water utilization efficiency. Together, these parameters were used to complement conventional measurements of soil water availability, Ψ, and gas-exchange traits.

2.6. Statistical Analysis

Statistical analyses were performed using SPSS Statistics 26.0 (IBM Corp., Armonk, NY, USA). The pot-level mean was used as the independent observation. Each species-by-habitat

combination had four replicate pots ($n = 4$), and the same pots were measured repeatedly across the nine drought stages. Because the primary aim was to describe temporal patterns within each species-by-habitat combination, one-way ANOVA followed by Tukey's multiple comparison test was used to compare drought stages within each combination. These analyses were descriptive and did not explicitly model the repeated-measures structure; therefore, p values should be interpreted with caution. No full factorial species-by-habitat-by-drought-stage interaction was tested. Statistical significance was set at $p < 0.05$.

Pearson correlation analysis was performed to evaluate the relationships among soil water content, leaf water potential, intracellular water-related parameters, and photosynthetic traits. Correlation coefficients were describe the direction and strength of associations.

Principal component analysis (PCA) was used as an exploratory method to visualize multivariate patterns. The PCA was performed on treatment-level mean values for each species-by-habitat-by-drought-stage combination. Variables were standardized to Z-score. The number of principal components retained was based on eigenvalues greater than 1. PCA was used for exploratory visualization and does not imply causality or mechanism. The 95% confidence ellipses in the PCA biplot were used descriptively to visualize group dispersion and should be interpreted with caution given the sample size ($n = 4$ per species-by-habitat combination; 36 treatment-level observations in total). PCA was conducted in SPSS 26.0 (IBM Corp., Armonk, NY, USA), and the resulting ordination plots were prepared using OriginPro 2021 (OriginLab, Northampton, MA, USA).

3. Results

3.1. Progressive Decline in SWC

SWC declined progressively throughout the 16-day drought treatment in both RO and NRO habitats (Table 1). By D16, SWC in the *B. papyrifera* L. plots had decreased by 92.7% and 90.6% in the RO and NRO habitats, respectively, while corresponding reductions of 90.8% and 91.9% were recorded for *M. alba* L. At the final stage (D16), RO and NRO habitats within the same species shared the same lowercase letters (Table 1), indicating that no statistically significant differences in SWC were detected between the two habitats for either species ($p > 0.05$) under the experimental conditions. However, this absence of a detected difference does not demonstrate equivalence between the habitats, especially given the sample size ($n = 4$ per species-by-habitat combination).

Table 1. Dynamics of soil water content with drought duration in two habitats.

Day	*B. papyrifera* L.		*M. alba* L.	
	RO	NRO	RO	NRO
0	0.4340 ± 0.1 a	0.4188 ± 0.01 a	0.4307 ± 0.0 a	0.3985 ± 0.0 a
2	0.3437 ± 0.01 b	0.3312 ± 0.08 b	0.3200 ± 0.0 b	0.3268 ± 0.0 b
4	0.2122 ± 0.1 cd	0.2482 ± 0.06 c	0.1090 ± 0.0 c	0.1100 ± 0.0 c
6	0.1385 ± 0.0 ef	0.1763 ± 0.1 de	0.1070 ± 0.0 c	0.0993 ± 0.0 c
8	0.0977 ± 0.0 fgh	0.1177 ± 0.0 fg	0.0893 ± 0.0 cd	0.0670 ± 0.0 d
10	0.0713 ± 0.0 ghi	0.0847 ± 0.0 ghi	0.080 ± 0.0 cde	0.0665 ± 0.0 d
12	0.0607 ± 0.0 hi	0.0725 ± 0.0 ghi	0.0698 ± 0.0 de	0.0578 ± 0.0 de
14	0.051 ± 0.0 hi	0.057 ± 0.01 hi	0.0573 ± 0.0 ef	0.0430 ± 0.0 ef
16	0.0315 ± 0.0 i	0.0392 ± 0.0 i	0.0398 ± 0.0 f	0.0323 ± 0.0 f

Values are means ± SEs ($n = 4$). Different lowercase letters within the same species–habitat combination indicate significant differences among drought durations at $p < 0.05$. RO, rock outcrop; NRO, non-rock outcrop.

3.2. Species-Specific Responses of Leaf Water Potential

Ψ became progressively more negative with drought progression in both species (Figure 2). However, the temporal patterns differed markedly between species.

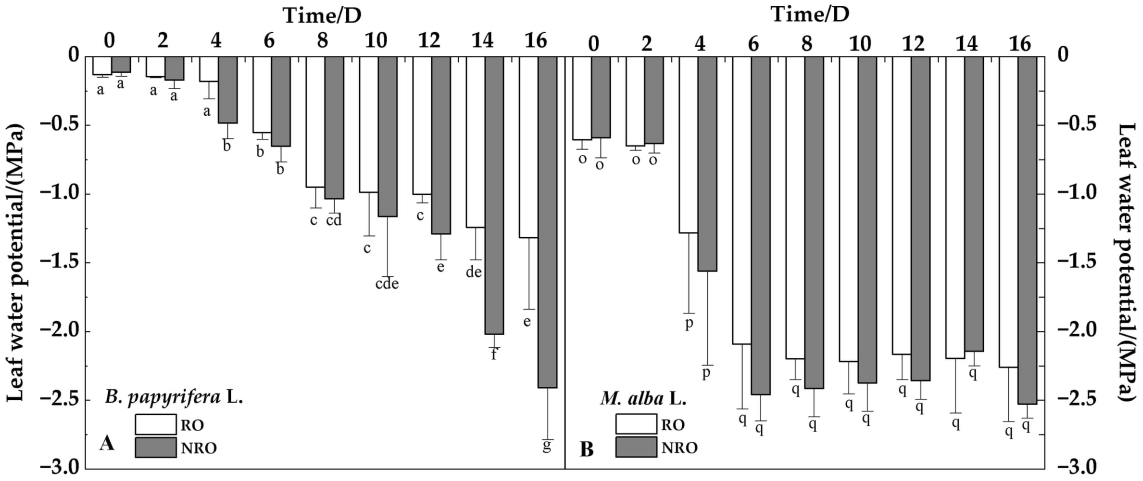


Figure 2. Leaf water potential (Ψ) under progressive drought. Values are means ± SE (n = 4). Different lowercase letters indicate significant differences among drought stages ($p < 0.05$). (**A**) *B. papyrifera* L.; (**B**) *M. alba* L.

In *B. papyrifera* L., Ψ declined gradually throughout the experimental period. In the RO habitat, Ψ decreased to −1.32 ± 0.52 MPa by D16, whereas a much lower value (−2.41 ± 0.38 MPa) was recorded in the NRO habitat (Figure 2A), indicating a more severe water deficit in NRO habitat at the late stage.

In contrast, *M. alba* L. exhibited a precipitous decline in Ψ during the early stages of drought, particularly in the NRO habitat, where Ψ dropped to −1.56 ± 0.68 MPa by D4 (Figure 2B). The magnitude of this decline was more than three times that observed in *B. papyrifera* L. at the same time point (−0.48 ± 0.12 MPa). By D16, Ψ in both RO and NRO habitats of *M. alba* L. fell below −2.2 MPa, reaching the lowest observed value of −2.53 ± 0.10 MPa in NRO.

Overall, *M. alba* L. exhibited a steeper and earlier decline in Ψ during progressive drought than *B. papyrifera* L., particularly during the initial 4–6 days of water deficit.

3.3. Intracellular Water Dynamics Under Progressive Drought

Intracellular water dynamics changed progressively during drought, although the temporal responses differed among parameters and between species (Figure 3). Overall, IWHC and IWTR generally declined during the early to middle stages of drought, whereas IWHT increased continuously. IWUE exhibited comparatively smaller changes and showed species-specific temporal patterns.

In *B. papyrifera* L., IWHC generally declined throughout drought. In the RO habitat, IWHC decreased from 0.68 ± 0.10 at D0 to 0.07 ± 0.04 at D8, followed by a slight increase to 0.20 ± 0.05 at D16 (Figure 3A). In the NRO habitat, IWHC declined from 0.50 ± 0.19 at D0 to 0.13 ± 0.13 at D16. IWTR decreased rapidly during the early stages and approached zero by D6 in both habitats (Figure 3C). In contrast, IWHT increased progressively throughout drought, whereas IWUE fluctuated only slightly during the experimental period (Figure 3E,G).

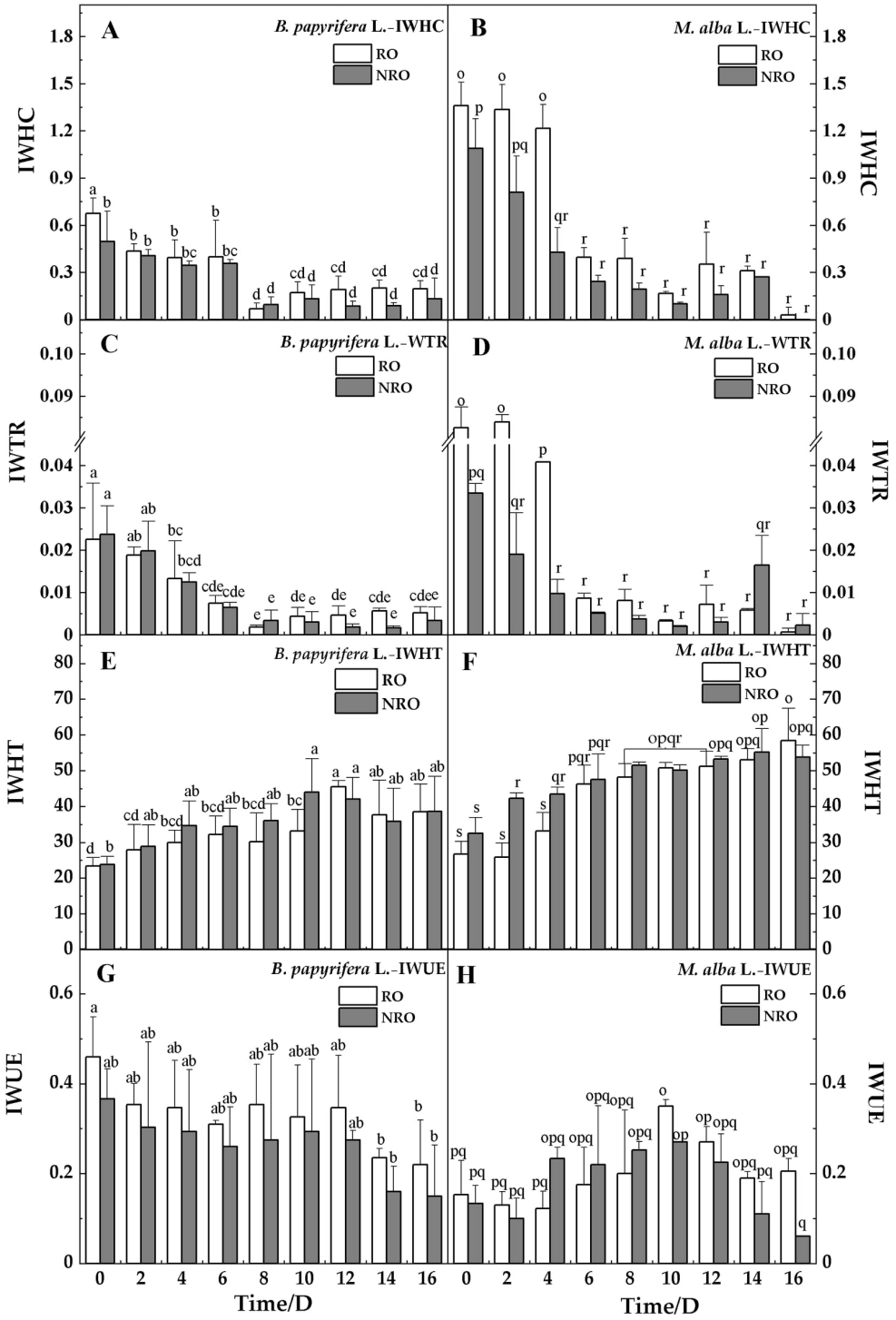


Figure 3. Intracellular water dynamics under progressive drought. (**A**,**B**) Intracellular water-holding capacity (IWHC); (**C**,**D**) intracellular water transport rate (IWTR); (**E**,**F**) intracellular water-holding time (IWHT); (**G**,**H**) intracellular water-use efficiency (IWUE). Values are means ± SE (n = 4). Different lowercase letters indicate significant differences among drought stages within each species–habitat combination ($p < 0.05$, a–e for *B. papyrifera* L., and o–s for *M. alba* L.).

In *M. alba* L., IWHC also declined progressively but decreased more sharply during the early drought stages. In the RO habitat, IWHC decreased from 1.36 ± 0.15 at D0 to 0.39 ± 0.06 at D6, while in the NRO habitat, it dropped from 1.09 ± 0.19 at D0 to 0.24 ± 0.04 at D6 (Figure 3B). IWTR also declined rapidly and approached zero by D6 in both habitats (Figure 3D). IWHT increased progressively throughout drought, whereas IWUE increased

during the middle stages of drought, reached its maximum at D10 in the RO habitat, and subsequently declined as drought progressed (Figure 3F,H). Overall, intracellular water dynamics exhibited distinct species-specific temporal responses during drought progression.

3.4. Photosynthetic Responses to Progressive Drought

Photosynthetic traits responded progressively to drought in both species (Figure 4). P_n, gsw, and E generally declined throughout drought progression, whereas WUE exhibited species-specific temporal patterns.

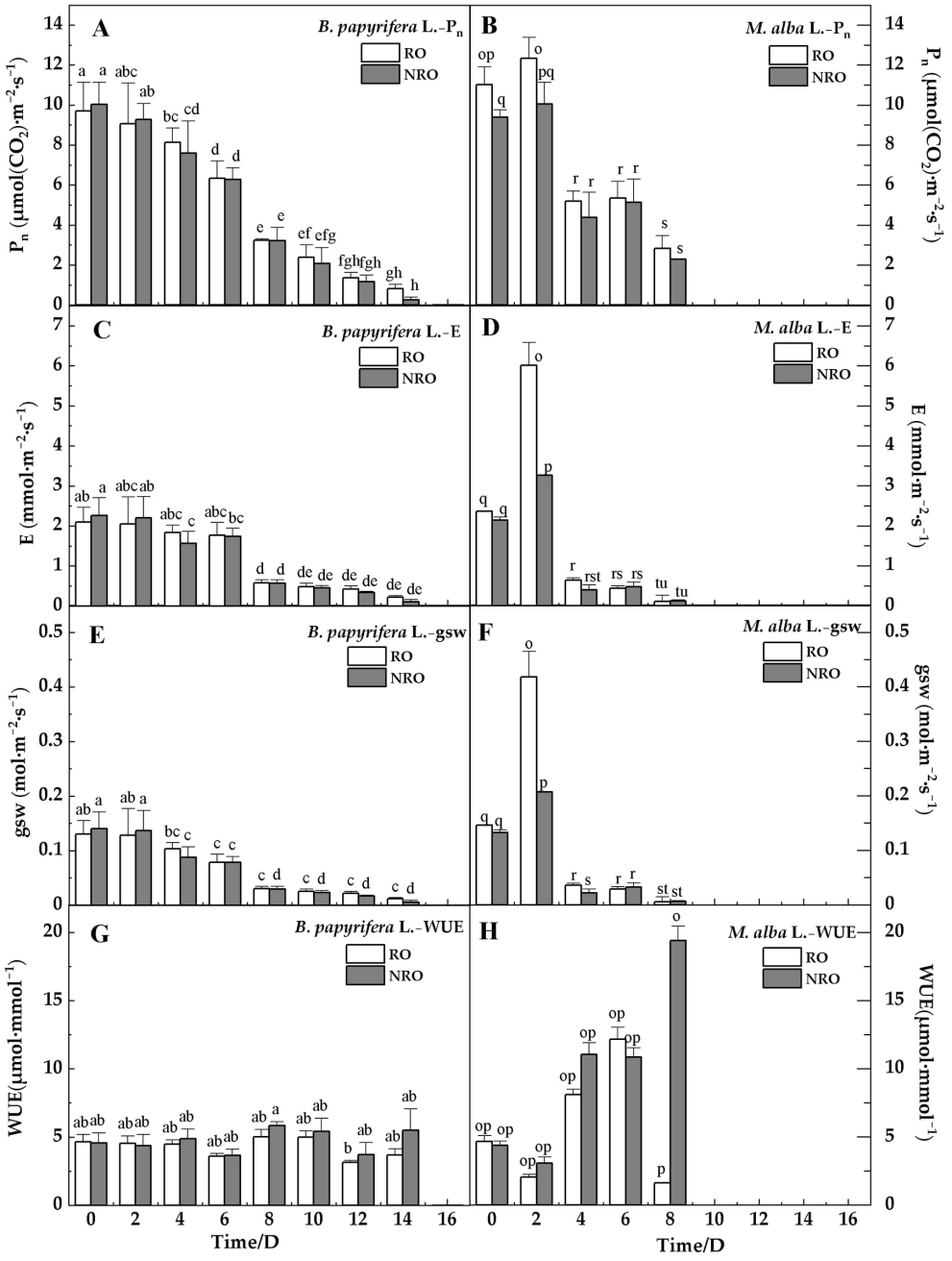


Figure 4. Photosynthetic responses under progressive drought. (**A**,**B**) Net photosynthetic rate (P_n); (**C**,**D**) transpiration rate (**E**); (**E**,**F**) stomatal conductance (gsw); (**G**,**H**) instantaneous water-use efficiency (WUE). Values are means ± SE ($n = 4$). Different lowercase letters indicate significant differences among drought stages within each species–habitat combination ($p < 0.05$, a–h for *B. papyrifera* L., and o–u for *M. alba* L.).

In *B. papyrifera* L., P_n decreased continuously from 9.70 ± 1.42 μmol CO_2 m^{-2} s^{-1} at D0 to near-zero or slightly negative values by D16 in both habitats (Figure 4A). gsw and E also declined progressively (Figure 4C,E). In the RO habitat, WUE increased to a peak of 5.02 ± 0.54 mmol mol^{-1} at D8, then declined, before recovering slightly at D14 (Figure 4G).

In *M. alba* L., P_n increased slightly during the initial stage of drought in both habitats, reaching 12.34 ± 1.03 μmol CO_2 m^{-2} s^{-1} at D2 in RO and 10.05 ± 1.09 μmol CO_2 m^{-2} s^{-1} at D2 in NRO, but subsequently declined rapidly to near zero by D8 (Figure 4B). E and gsw followed a similar pattern, with an initial transient increase at D2 followed by a sharp decline (Figure 4D,F). The WUE increased sharply and reached maximum values at D6 in the RO habitat (12.17 ± 0.88 mmol mol^{-1}) and at D8 in the NRO habitat (19.39 ± 4.05 mmol mol^{-1}), followed by a gradual decline toward the later stages of drought (Figure 4H).

Overall, *B. papyrifera* L. exhibited a more gradual decline in photosynthetic traits than *M. alba* L. during drought progression.

3.5. Correlations Between Intracellular Water Dynamics and Photosynthetic Traits

Pearson correlation analysis revealed significant relationships between intracellular water dynamics and photosynthetic traits in both species (Figure 5).

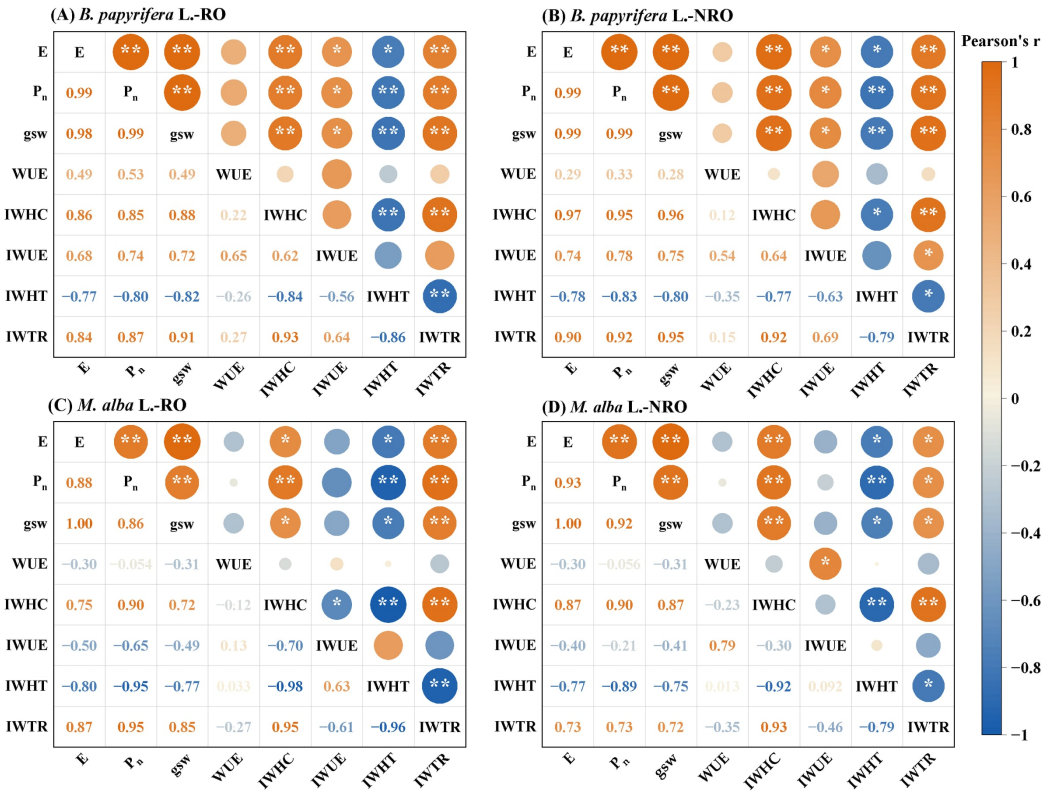


Figure 5. Pearson correlation matrix of intracellular water dynamics and photosynthetic traits. (**A**) *B. papyrifera* L. RO; (**B**) *B. papyrifera* L. NRO; (**C**) *M. alba* L. RO; (**D**) *M. alba* L. NRO. ** and * indicate significant correlations at $p < 0.01$ and $p < 0.05$, respectively (two-tailed).

In *B. papyrifera* L., P_n was positively correlated with IWHC (r = 0.85 in RO; r = 0.95 in NRO) and IWTR (r = 0.87 in RO; r = 0.92 in NRO), whereas negative correlations were observed with IWHT (r = −0.80 in RO; r = −0.83 in NRO). Similar patterns were observed for gsw, which showed strong positive correlations with IWHC (r = 0.88 in RO; r = 0.96 in NRO) and IWTR (r = 0.91 in RO; r = 0.95 in NRO), but negative correlations with IWHT (r = −0.82 in RO; r = −0.80 in NRO) (Figure 5A,B).

In *M. alba* L., P_n was positively correlated with IWHC (r = 0.90 in both RO and NRO) and IWTR (r = 0.95 in RO; r = 0.73 in NRO), whereas negative correlations were observed with IWHT (r = −0.95 in RO; r = −0.89 in NRO). Similarly, gsw was positively correlated with IWHC (r = 0.72 in RO; r = 0.87 in NRO) and IWTR (r = 0.85 in RO; r = 0.72 in NRO), and negatively correlated with IWHT (r = −0.77 in RO; r = −0.75 in NRO) (Figure 5C,D).

Across both species and habitats, IWHC and IWTR were consistently positively correlated with photosynthetic traits, whereas IWHT showed consistently negative correlations with P_n, gsw, and E (Figure 5).

3.6. Principal Component Analysis (PCA)

Principal component analysis (PCA) revealed distinct multivariate response patterns between *B. papyrifera* L. and *M. alba* L. along the first two principal components, which together explained 78.8% of the total variance (PC1 = 61.7%, PC2 = 17.1%) (Figure 6). PC1 was primarily associated with soil and leaf water status, photosynthetic activity, and intracellular water traits, with strong positive loadings from SWC, P_n, gsw, E, IWHC, and IWTR, whereas IWHT showed a negative loading on PC1. PC2 was characterized mainly by a strong positive loading of IWUE, together with negative loadings of IWTR and IWHC, while Ψ also showed a positive loading on PC2. Samples of *B. papyrifera* L. were mainly distributed in the positive regions of both PC1 and PC2, and were positioned closer to WUE, Ψ, and photosynthetic traits. In contrast, *M. alba* L. samples were mainly distributed in the negative region of PC1 and were positioned closer to IWHT, consistent with differences in the multivariate patterns of intracellular water-related traits between the two species. The 95% confidence ellipses showed limited overlap between the two species, descriptively illustrating differences in their multivariate physiological response patterns. These ellipses are used for visualization only and should be interpreted with caution because the sample size per group is limited (n = 4 per species-by-habitat combination; 36 treatment-level observations in total).

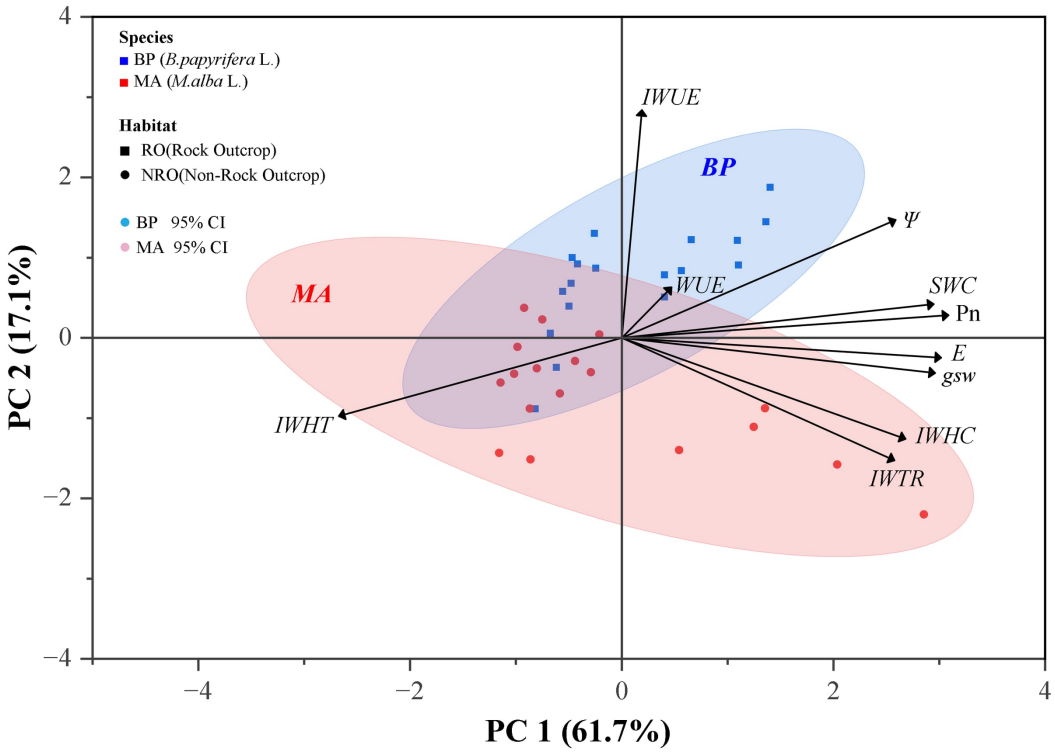


Figure 6. PCA of *B. papyrifera* L. (BP) and *M. alba* L. (MA) across RO and NRO habitats under nine progressive drought stages. Variables were standardized to z-scores, and PCA was performed on

treatment-level mean values for each species-by-habitat-by-drought-stage combination ($n = 4$ per species-by-habitat combination; 36 treatment-level observations in total). PC1 (61.7%) was primarily associated with soil and leaf water status, photosynthetic activity, and intracellular water traits; PC2 (17.1%) was mainly associated with IWUE and intracellular water transport- and water-holding-related traits. Symbols indicate species-by-habitat-by-drought-stage combinations; arrows represent variable loadings. Ellipses indicate 95% confidence ellipses for each species and are descriptive; they should be interpreted with caution given the limited sample size. PCA is exploratory and does not demonstrate causal mechanisms.

4. Discussion

4.1. Progressive Drought Alters Plant Water Status and Intracellular Water Dynamics

Progressive drought resulted in a marked decline in SWC throughout the 16-day experimental period, accompanied by increasingly negative Ψ in both *B. papyrifera* L. and *M. alba* L. These concurrent changes indicate a progressive deterioration of plant water status as soil water availability decreased. Such responses are consistent with established descriptions of drought physiology, in which declining soil water availability progressively alters leaf water status and physiological function [5,6].

This response is particularly relevant in karst ecosystems, where shallow and discontinuous soils, exposed bedrock, and strong spatial heterogeneity in soil–rock structures can constrain water storage and plant water availability [7–10]. Recent studies further indicate that water uptake and transpiration of woody plants in karst ecosystems vary with rooting depth and seasonal water availability, reflecting the importance of spatially and temporally heterogeneous water sources for plant water use [11]. Recent evidence also shows that root-zone soil moisture can buffer and delay vegetation responses to drought in karst landscapes, indicating that surface soil moisture alone may not fully represent the water available to plants [24]. Karst fissures may also mitigate the negative effects of drought on plant growth and photosynthetic physiology, further highlighting the potential buffering role of subsurface water resources in karst habitats [25]. Therefore, the progressive decrease in SWC observed in our experiment provides an appropriate environmental gradient for examining subsequent physiological responses.

However, the two species differed in the timing and magnitude of Ψ decline. *M. alba* L. exhibited an earlier and more pronounced decrease in Ψ during the initial stages of drought, whereas *B. papyrifera* L. maintained comparatively higher Ψ for a longer period. This interspecific difference is consistent with previous observations of contrasting dehydration responses in *M. alba* L. and *B. papyrifera* L. In detached-leaf dehydration experiments, intracellular water availability of *M. alba* L. declined earlier than that of *B. papyrifera* L., suggesting greater sensitivity of *M. alba* L. to dehydration [19]. The present results extend this observation from short-term leaf dehydration to a progressive soil-drought context and suggest that the difference between the two species is also expressed at the whole-leaf water-status level.

The relatively slower decline in Ψ in *B. papyrifera* L. may indicate a greater capacity to maintain leaf water status during progressive soil drying, whereas the earlier decline in *M. alba* L. indicates a more rapid adjustment to decreasing water availability. Similar interspecific differences in water-use and drought-response strategies have been documented in karst vegetation [26,27]. However, because root water uptake, xylem hydraulic conductance, and water sources were not directly measured in the present study, these differences should not be attributed to a specific hydraulic mechanism.

Changes in leaf water status were accompanied by marked changes in intracellular water dynamics. IWHC and IWTR generally decreased during drought, whereas IWHT generally increased. This contrasting response among intracellular water parameters is

important because it indicates that intracellular water dynamics did not respond as a single physiological process. Instead, different components of intracellular water status exhibited distinct temporal trajectories during progressive dehydration.

Previous studies using physiological impedance measurements have shown that electrical parameters can provide information on plant water status and leaf water content [28]. Electrical parameters have also been linked to changes in intracellular water metabolism and physiological state, supporting their use as indirect indicators of water-related physiological processes [29]. Xing et al. [18] demonstrated that physiological impedance-derived intracellular water transport parameters changed with water supply and were associated with Ψ, photosynthesis, and WUE. More directly relevant to the present study, Yu et al. [19] demonstrated species-specific responses of intracellular water metabolism in *M. alba* L. and *B. papyrifera* L. under water shortage. The consistency between those observations and the present species differences strengthens the physiological relevance of the impedance-derived parameters used here.

The increase in IWHT likely reflects a shift in the temporal characteristics of intracellular water dynamics, rather than being direct evidence of enhanced water storage or active retention (cellular water content and membrane properties were not independently measured in this study). Instead, IWHT may offer complementary information on the temporal dimension of intracellular water regulation under progressive drought. Overall, the concurrent decline in IWHC and IWTR and increase in IWHT suggest that progressive drought was associated with changes in multiple aspects of impedance-derived intracellular water dynamics, rather than a uniform change in intracellular water status. Together with the species-specific trajectories of Ψ, these findings suggest that *B. papyrifera* L. and *M. alba* L. differed in the timing and coordination of water-status adjustment during progressive drought. By characterizing these changes across nine drought stages, the present study provides a time-resolved assessment of the variation in intracellular water-related parameters alongside leaf water potential during progressive drought.

4.2. Intracellular Water Dynamics Are Associated with Photosynthetic Adjustment Under Progressive Drought

Progressive drought resulted in substantial declines in P_n, gsw, and E in both species. These responses are consistent with the established effects of water limitation on stomatal regulation and photosynthetic carbon assimilation [17,30]. Under progressive drought, stomatal closure can reduce transpiration and protect plant water status, but prolonged or severe water limitation can subsequently impose additional non-stomatal constraints on photosynthesis [30].

An important result of the present study is that the decline in photosynthetic performance occurred concurrently with changes in intracellular water dynamics. IWHC and IWTR decreased as P_n, gsw, and E declined, and correlation analysis showed positive associations between IWHC/IWTR and photosynthetic traits. Recent studies have likewise demonstrated that changes in leaf intracellular water characteristics are closely associated with photosynthetic performance and water-use efficiency under different water availability conditions [31,32]. Consistent with this relationship, electrical parameters have also been reported to be associated with photosynthetic characteristics under simulated karst drought, supporting the relevance of electrical measurements for characterizing physiological responses to water limitation [33]. Xing et al. [31] showed that changes in leaf intracellular retained water and intracellular water transport were associated with changes in transpiration and instantaneous water-use efficiency under different water supply strategies. More recently, Quispe-Puma et al. [32] reported coordinated changes in leaf intracellular water characteristics and photosynthetic responses during drought stress.The positive relation-

ships between IWHC/IWTR and photosynthetic traits observed here indicate coordinated responses, but correlation does not imply causation; direct regulatory links remain to be tested. The strong positive associations observed in *B. papyrifera* L. are nevertheless physiologically informative. They suggest that the maintenance of intracellular water-related properties was accompanied by the maintenance of gas exchange during the earlier stages of drought. In contrast, the earlier decline in IWHC and IWTR in *M. alba* L. occurred together with earlier declines in P_n, gsw, and E. Thus, the temporal coordination between intracellular water parameters and photosynthetic traits differed between the two species.

The response of IWUE provides an additional dimension of intracellular water dynamics. In *M. alba* L., IWUE increased transiently during the intermediate drought stages before declining at later stages. Because IWUE was derived from impedance-based physiological parameters, its variation should be interpreted as changes in intracellular water-use characteristics rather than as changes in gas-exchange-derived WUE [18,19]. The transient increase in IWUE may reflect an adjustment of intracellular water dynamics during the intermediate stages of drought, although the specific physiological basis of this response requires further investigation.

In contrast, instantaneous WUE was calculated from gas-exchange measurements as the ratio of P_n to E. The increase in WUE observed during the intermediate stages therefore reflects the balance between carbon assimilation and transpirational water loss and does not necessarily indicate improved photosynthetic performance.

The contrasting response of IWHT provides an additional dimension. IWHT increased while P_n, gsw, and E declined, and IWHT showed negative associations with these photosynthetic traits. However, this negative relationship likely reflects their opposite temporal trends during drought progression rather than a direct inhibitory effect of IWHT on photosynthesis. Recent studies of plant electrical impedance spectroscopy indicate that impedance-related parameters can provide information on plant water status and physiological condition, but their physiological interpretation depends on the measured tissue, frequency range, equivalent-circuit model, and measurement context [28,34]. Therefore, the present impedance-derived parameters should be interpreted as physiological indicators associated with intracellular water dynamics rather than direct measurements of leaf hydraulic conductance.

Together, these results indicate that intracellular water dynamics and photosynthetic performance exhibited coordinated temporal changes during progressive drought. Integrating impedance-derived intracellular water parameters with conventional water-status and gas-exchange measurements therefore provides a multidimensional characterization of drought responses.

4.3. Species-Specific Coordination of Intracellular Water Dynamics During Progressive Drought

Although both *B. papyrifera* L. and *M. alba* L. exhibited broadly similar directional responses to drought, their temporal trajectories differed substantially. *M. alba* L. showed earlier reductions in Ψ, IWHC, IWTR, P_n, gsw, and E, whereas *B. papyrifera* L. exhibited a more gradual decline in these traits. This difference in response timing, rather than simply the final magnitude of change, appears to be a major distinction between the two species.

The importance of response timing is supported by previous studies on these two Moraceae species. Xing et al. [35] found that intracellular water availability in *M. alba* L. decreased earlier than in *B. papyrifera* L. during controlled leaf dehydration, whereas *B. papyrifera* L. showed greater adjustment of leaf structure during water loss. Yu et al. [19] subsequently reported differential intracellular water metabolism between the two species under contrasting water availability. More broadly, recent studies have shown that species-specific differences in hydraulic regulation and drought tolerance can involve differences

in the timing and coordination of water-status adjustment [21,36]. The present results are consistent with these studies and extend them by showing that the species difference persists across a 16-day progressive soil-drought gradient.

In *B. papyrifera* L., photosynthetic activity declined more gradually despite substantial changes in IWHC and IWTR. This suggests that the relatively gradual decline in photosynthetic performance under progressive drought was associated with the coordinated response of multiple physiological traits rather than with the maintenance of any single intracellular water parameter. Previous comparative work on *B. papyrifera* L. and *M. alba* L. has also documented species differences in photosynthetic characteristics associated with adaptation to karst soil conditions [37]. The relatively stable IWUE and progressive increase in IWHT accompanied the gradual changes in photosynthetic performance in *B. papyrifera* L. during drought progression. These patterns suggest that intracellular water-related parameters and photosynthetic traits changed in a coordinated manner, although the present data do not establish a specific water-use strategy or hydraulic mechanism [20].

By contrast, *M. alba* L. showed an earlier and stronger physiological response. Its earlier decline in Ψ was accompanied by earlier reductions in IWHC and IWTR and subsequent reductions in P_n, gsw, and E. The transient increase in IWUE suggests a temporary adjustment in intracellular water-use characteristics, but the subsequent decline suggests that the transient adjustment was not sustained under severe drought, when photosynthetic performance also declined markedly. In contrast, the increase in gas-exchange-derived WUE can coexist with reduced photosynthetic performance when transpiration declines more strongly than carbon assimilation.

The PCA further revealed clear species-specific multivariate patterns. PC1 and PC2 explained 61.7% and 17.1% of the total variation, respectively, accounting for 78.8% of the variation. *B. papyrifera* L. was more strongly associated with Ψ, P_n, gsw, E, WUE, and IWUE, whereas *M. alba* L. was more closely associated with IWHT. This pattern indicates that the two species occupied different regions of multivariate physiological space during drought progression. Importantly, the PCA does not demonstrate different hydraulic mechanisms; rather, it identifies different combinations of physiological traits associated with the two species. These PCA patterns are exploratory and should be interpreted as hypothesis-generating rather than confirmatory.

This interpretation is consistent with studies showing substantial interspecific variation in drought-response strategies among woody plants. In karst ecosystems, differences in water acquisition, root distribution, Ψ, and hydraulic safety margins can contribute to contrasting drought vulnerability among co-occurring species [22,27]. Recent evidence further indicates that hydraulic trait variability and conservative stomatal regulation can facilitate species persistence across heterogeneous karst water environments [38]. The present study adds intracellular water-related traits to this framework and suggests that these parameters may help resolve physiological differences that are not fully captured by conventional measurements of Ψ and gas exchange.

Collectively, the results indicate that *B. papyrifera* L. and *M. alba* L. exhibited different temporal patterns of physiological responses to drought. *B. papyrifera* L. showed comparatively gradual changes in leaf water status, intracellular water dynamics, and photosynthesis, whereas *M. alba* L. exhibited earlier and more pronounced changes. The comparatively gradual decline in these traits in *B. papyrifera* L. suggests a slower physiological response to progressive drought under the conditions tested. These patterns reflect species-specific drought responses, although the present data do not establish the underlying hydraulic or cellular mechanisms. The observed differences may be relevant to how the two species respond to declining soil water availability in karst habitats.

From an applied perspective, integrating intracellular water-related parameters with conventional physiological measurements may provide a basis for monitoring plant responses to soil drying. This integrated approach may help characterize changes in plant physiological status during progressive drought and provide a basis for further evaluating species suitability for drought-prone environments and supporting irrigation management. However, field validation and assessments of plant growth and survival are needed before these findings can inform specific recommendations for species selection or water-management practices.

4.4. IWHT as a Potential Temporal Indicator of Intracellular Water Regulation During Drought

Among the intracellular water-related parameters examined, IWHT showed the most distinctive response pattern. Whereas IWHC and IWTR generally decreased with progressive drought, IWHT increased. Moreover, IWHT showed negative associations with P_n, gsw, and E and was more closely associated with *M. alba* L. in the PCA.

This contrasting behavior suggests that IWHT may reflect a temporal dimension of intracellular water dynamics that is not fully represented by IWHC or IWTR. Recent studies using plant bioimpedance and electrical impedance spectroscopy have shown that impedance-derived parameters can provide information on leaf water status and physiological responses under water deficit [28,39]. Yu et al. [19] further demonstrated that intracellular water metabolism derived from electrophysiological information differed between *M. alba* L. and *B. papyrifera* L., providing a direct precedent for interpreting species-specific responses in the present study.

The increase in IWHT during drought may indicate a change in the temporal characteristics of intracellular water dynamics as water availability declines, but it would be premature to interpret this pattern as direct evidence of enhanced intracellular water retention, as IWHT is derived from impedance-based physiological parameters and cellular water content/membrane permeability were not independently measured. Similarly, the negative correlations between IWHT and photosynthetic traits likely reflect their opposite temporal responses to drought rather than a direct inhibitory effect. Rather, IWHT may serve as an indicator of the physiological state accompanying progressive dehydration.

The PCA suggests that IWHT may contribute to the multivariate differentiation between the two species. Its association with *M. alba* L. in the PCA indicates that IWHT may provide information complementary to Ψ, WUE, and conventional gas-exchange traits. This interpretation is consistent with recent evidence that drought responses are multidimensional and involve coordinated variation across multiple physiological and functional traits [40,41].

Accordingly, we consider IWHT a potential temporal indicator rather than an established hydraulic trait or a validated predictor of drought tolerance. It may complement conventional measurements by providing information on the temporal dimension of intracellular water dynamics. Future studies combining IWHT with direct measurements of leaf hydraulic conductance, cellular water status, membrane properties, and stomatal responses are needed to test whether IWHT can serve as a predictive indicator across species and drought environments.

4.5. Conceptual Synthesis of Intracellular Water Regulation During Progressive Drought

The results support a conceptual framework in which progressive soil drying is associated with coordinated changes in plant water status, intracellular water dynamics, and photosynthetic performance (Figure 7). As SWC declined, Ψ became increasingly negative, while IWHC and IWTR generally decreased and IWHT increased. These changes occurred concurrently with declines in P_n, gsw, and E.

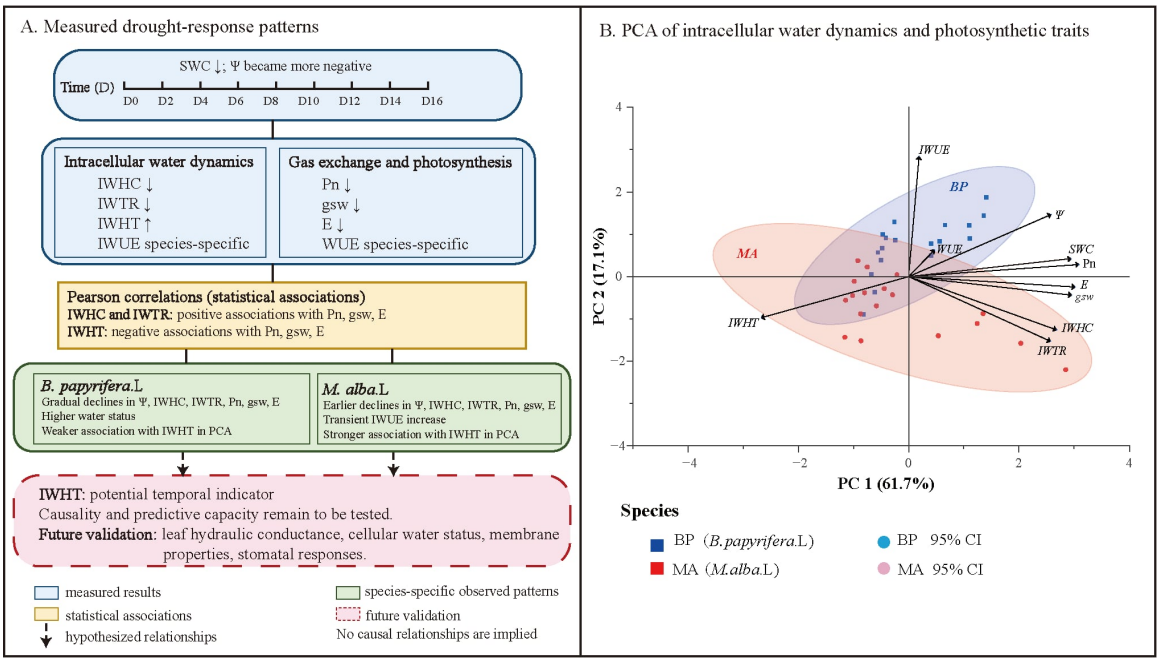


Figure 7. Conceptual framework and multivariate analysis of intracellular water dynamics under progressive drought. (**A**) The framework distinguishes measured results (solid blue boxes), statistical associations (solid yellow box), species-specific observed patterns (solid green boxes), and hypothesized relationships (dashed pink box). Solid connecting lines indicate analytical flow without implying causality. Dashed arrows indicate hypothesized relationships requiring future validation. No causal relationships are implied. (**B**) PCA of intracellular water dynamics and photosynthetic traits (see Figure 6 for details). PCA is exploratory and does not demonstrate causal mechanisms.

The major contribution of this framework is that it incorporates intracellular water dynamics into the conventional soil–plant water status–photosynthesis continuum. Previous studies have established strong relationships among soil water availability, Ψ, stomatal regulation, and photosynthetic limitation under drought [17,25]. The present results suggest that changes in intracellular water-related properties occur within the same drought-response trajectory and provide additional physiological information.

The two species differed in the temporal expression of this response. *B. papyrifera* L. maintained comparatively higher Ψ and exhibited more gradual changes in intracellular water dynamics and photosynthetic performance, whereas *M. alba* L. showed earlier declines in Ψ, IWHC, IWTR, and gas-exchange traits and a stronger association with IWHT. These species-specific trajectories are consistent with previous studies of Moraceae dehydration and intracellular water metabolism [18,19], as well as with broader evidence of species-specific drought responses in karst vegetation [22,27] and recent evidence that woody species can differ substantially in the coordination of stomatal, hydraulic, and photosynthetic responses to water limitation [41].

Importantly, Figure 7 is intended as a conceptual synthesis of observed temporal patterns and statistical associations rather than as a demonstrated causal pathway. The present study did not directly quantify root water uptake, xylem hydraulic conductance, leaf hydraulic conductance, cellular water content, osmotic adjustment, or non-stomatal photosynthetic limitations; therefore, these mechanisms cannot be resolved from the current data. Within this conceptual framework, IWHT emerges as a promising candidate indicator of the temporal dimension of intracellular water regulation. Recent bioimpedance research has shown that impedance-derived parameters can provide information on leaf water status and may capture physiological changes associated with water stress, although their interpretation depends on the measurement and modelling framework [28,34,39]. How-

ever, this interpretation requires validation across additional species, drought intensities, developmental stages, and field conditions.

Overall, the present study indicates that progressive drought is associated with coordinated but species-specific changes in soil water availability, leaf water status, intracellular water dynamics, and photosynthetic performance. The integration of physiological impedance-derived intracellular water parameters with conventional drought indicators provides a potentially useful framework for resolving the temporal organization of plant responses to water limitation in karst woody plants.

5. Conclusions

Progressive drought was accompanied by coordinated changes in plant water status, intracellular water dynamics, and photosynthetic performance in *B. papyrifera* L. and *M. alba* L. Declining soil water availability was associated with increasingly negative leaf water potential, reductions in IWHC and IWTR, an increase in IWHT, and declines in P_n, gsw, and E.

The major distinction between the two species lay in the timing of physiological responses. *M. alba* L. showed earlier declines in Ψ, intracellular water-related parameters, and photosynthetic traits, whereas *B. papyrifera* L. maintained comparatively higher water status and exhibited more gradual physiological adjustment, particularly in the rock outcrop habitat. These patterns suggest contrasting temporal modes of physiological adjustment during progressive drought.

Correlation and PCA analyses indicated that intracellular water dynamics were associated with photosynthetic responses and were involved in the multivariate differentiation of the two species. As an impedance-based temporal parameter, IWHT was associated with species-specific drought responses and may provide complementary information on the temporal dimension of intracellular water dynamics. However, this study does not establish a causal relationship between IWHT and drought tolerance or photosynthetic performance, nor does it validate IWHT as a predictive indicator of these traits.

Overall, integrating intracellular water-related parameters with conventional physiological measurements provides a potentially useful framework for characterizing drought responses in karst woody plants. However, the physiological interpretation and predictive value of IWHT still require further validation through direct measurements of cellular water status and leaf hydraulic properties, and through testing across additional species and drought intensities under field conditions.

Author Contributions: L.L. and Y.W. conceived and designed the experiments; L.L. performed the experiments and analyzed the data; L.L. wrote the original draft; Y.W. reviewed and edited the manuscript. All authors have read and agreed to the published version of the manuscript.

Funding: This research was funded by Qiankehe foundation MS [2026] 724.

Data Availability Statement: The data supporting the findings of this study are available from the corresponding author upon reasonable request.

Acknowledgments: The author would like to express his sincere gratitude to Dong Li, who made a significant contribution to the analysis, drafting and revision of this study. Whilst drafting this manuscript, the author also utilised ChatGPT-4 (OpenAI) to assist with polishing the language and enhancing the clarity and logical coherence of the text. The author has reviewed and edited the generated content and assumes full responsibility for the content of this publication.

Conflicts of Interest: The authors declare no conflicts of interest.

Abbreviations

The following abbreviations are used in this manuscript:

SWC	Soil water content
Z	Total impedance
Cm	Membrane capacitance
Rm	Membrane resistance
Ro	Extracellular resistance
Ri	Intracellular resistance
Xcm	Membrane capacitive
XLm	Inductive reactance
RO	Rock outcrop
NRO	Non-rock outcrop
IWHC	Intracellular water-holding capacity
IWTR	Intracellular water transport rate
IWHT	Intracellular water-holding time
IWUE	Intracellular water-use efficiency
P_n	Net photosynthetic rate
E	Transpiration rate
gsw	Stomatal conductance
WUE	Instantaneous water-use efficiency

References

1. Sato, H.; Mizoi, J.; Shinozaki, K.; Yamaguchi-Shinozaki, K. Complex plant responses to drought and heat stress under climate change. *Plant J*. **2024**, *117*, 1873–1892. [CrossRef]
2. Ali, S.; Mir, R.A.; Haque, M.A.; Danishuddin; Almalki, M.A.; Alfredan, M.; Khalifa, A.; Mahmoudi, H.; Shahid, M.; Tyagi, A.; et al. Exploring physiological and molecular dynamics of drought stress responses in plants: Challenges and future directions. *Front. Plant Sci*. **2025**, *16*, 1565635. [CrossRef]
3. Jiao, W.; Wang, L.; Smith, W.K.; Chang, Q.; Wang, H.; D'Odorico, P. Observed increasing water constraint on vegetation growth over the last three decades. *Nat. Commun*. **2021**, *12*, 3777. [CrossRef]
4. Joshi, J.; Stocker, B.D.; Hofhansl, F.; Zhou, S.; Dieckmann, U.; Prentice, I.C. Towards a unified theory of plant photosynthesis and hydraulics. *Nat. Plants* **2022**, *8*, 1304–1316. [CrossRef]
5. Dos Santos, T.B.; Ribas, A.F.; de Souza, S.G.H.; Budzinski, I.G.F.; Domingues, D.S. Physiological Responses to Drought, Salinity, and Heat Stress in Plants: A Review. *Stresses* **2022**, *2*, 113–135. [CrossRef]
6. Cao, Y.; Yang, W.; Ma, J.; Cheng, Z.; Zhang, X.; Liu, X.; Wu, X.; Zhang, J. An integrated framework for drought stress in plants. *Int. J. Mol. Sci*. **2024**, *25*, 9347. [CrossRef]
7. Ning, J.; Liu, X.; Wu, X.; Yang, H.; Ma, J.; Cao, J. The Effect of Bedrock Differences on Plant Water Use Strategies in Typical Karst Areas of Southwest China. *Land* **2023**, *12*, 12. [CrossRef]
8. Leite, P.A.M.; Rempe, D.M.; McInnes, K.J.; Schmidt, L.M.; Walker, J.W.; Olariu, H.G.; Wilcox, B.P. Trees enhance rock moisture storage: A major pool in karst drylands and crucial during droughts. *Water Resour. Res*. **2025**, *61*, e2024WR038692. [CrossRef]
9. Li, Y.; Wang, S.; Peng, T.; Zhao, G.; Dai, B. Hydrological characteristics and available water storage of typical karst soil in SW China under different soil–rock structures. *Geoderma* **2023**, *438*, 116633. [CrossRef]
10. Zhu, X.; Liu, H.; He, W.; Wu, L.; Liu, F. Regolith water storage patterns determine vegetation productivity in global karst regions. *Geoderma* **2023**, *430*, 116292. [CrossRef]
11. Behzad, H.M.; Arif, M.; Duan, S.; Kavousi, A.; Cao, M.; Liu, J.; Jiang, Y. Seasonal Variations in Water Uptake and Transpiration for Plants in a Karst Critical Zone in China. *Sci. Total Environ*. **2023**, *860*, 160424. [CrossRef]
12. Zhou, Q.; Luo, Y.; Shi, C.; Li, Y. Hydrological effects of vegetation restoration in karst areas research: Progress and challenges. *Trans. Earth Environ. Sustain*. **2023**, *1*, 177–204. [CrossRef]
13. Ding, Y.; Nie, Y.; Chen, H.; Wang, K.; Querejeta, J.I. Water uptake depth is coordinated with leaf water potential, water-use efficiency and drought vulnerability in karst vegetation. *New Phytol*. **2021**, *229*, 1339–1353. [CrossRef]
14. Rodriguez-Dominguez, C.M.; Forner, A.; Martorell, S.; Choat, B.; Lopez, R.; Peters, J.M.R.; Pfautsch, S.; Mayr, S.; Carins-Murphy, M.R.; McAdam, S.A.M.; et al. Leaf water potential measurements using the pressure chamber: Synthetic testing of assumptions towards best practices for precision and accuracy. *Plant Cell Environ*. **2022**, *45*, 2037–2061. [CrossRef]
15. Busch, F.A.; Ainsworth, E.A.; Amtmann, A.; Cavanagh, A.P.; Driever, S.M.; Ferguson, J.N.; Kromdijk, J.; Lawson, T.; Leakey, A.D.B.; Matthews, J.S.A.; et al. A guide to photosynthetic gas exchange measurements: Fundamental principles, best practice and potential pitfalls. *Plant Cell Environ*. **2024**, *47*, 3344–3364. [CrossRef]

16. Chen, S.; ten Tusscher, K.H.W.J.; Sasidharan, R.; Dekker, S.C.; de Boer, H.J. Parallels between drought and flooding: An integrated framework for plant eco-physiological responses to water stress. *Plant Environ. Interact.* **2023**, *4*, 175–187. [CrossRef]
17. Zahra, N.; Hafeez, M.B.; Kausar, A.; Al Zeidi, M.; Asekova, S.; Siddique, K.H.M.; Farooq, M. Plant photosynthetic responses under drought stress: Effects and management. *J. Agron. Crop Sci.* **2023**, *209*, 651–672. [CrossRef]
18. Xing, D.; Mao, R.; Li, Z.; Wu, Y.; Qin, X.; Fu, W. Leaf intracellular water transport rate based on physiological impedance: A possible role of leaf internal retained water in photosynthesis and growth of tomatoes. *Front. Plant Sci.* **2022**, *13*, 845628. [CrossRef]
19. Yu, R.; Wu, Y.; Xing, D. The Differential Response of Intracellular Water Metabolism Derived from Intrinsic Electrophysiological Information in *Morus alba* L. and *Broussonetia papyrifera* (L.) Vent. Subjected to Water Shortage. *Horticulturae* **2022**, *8*, 182. [CrossRef]
20. Da Sois, L.; Mencuccini, M.; Castells, E.; Sanchez-Martinez, P.; Martínez-Vilalta, J. How are physiological responses to drought modulated by water relations and leaf economics' traits in woody plants? *Agric. Water Manag.* **2024**, *291*, 108613. [CrossRef]
21. Huang, D.-L.; Zhang, F.; Qie, Y.-D.; Wang, Y.-Q.; Wan, C.-Y.; Yu, J.-R.; Zhang, J.; Gan, J.-X.; Zhu, S.-D. Vulnerability segmentation is vital to hydraulic strategy of tropical–subtropical woody plants. *J. Ecol.* **2024**, *112*, 2798–2812. [CrossRef]
22. Williams, J.; Stella, J.C.; Singer, M.B.; Lambert, A.M.; Voelker, S.L.; Drake, J.E.; Friedman, J.M.; Pelletier, L.; Kui, L.; Roberts, D.A. Seasonal and species-level water-use strategies and groundwater dependence in dryland riparian woodlands during extreme drought. *Water Resour. Res.* **2024**, *60*, e2023WR035928. [CrossRef]
23. Fang, L.; Wu, Y.; Zhang, C.; Zhang, S. Leaf electrophysiological readouts reveal bicarbonate-associated shifts in early water-deficit response modes in *Broussonetia papyrifera* and *Morus alba*. *Plant Signal. Behav.* **2026**, *21*, 2657093. [CrossRef]
24. Liu, Y.; Lian, J.; Nie, Y.; Wang, K.; Chen, H. The role of root-zone soil moisture in delaying vegetation responses to drought: Comparative insights from karst and non-karst areas. *J. Hydrol.* **2025**, *663*, 134216. [CrossRef]
25. Luo, J.; Luo, W.-X.; Liu, J.-T.; Wang, Y.-J.; Li, Z.-F.; Tao, J.-P.; Liu, J.-C. Karst fissures mitigate the negative effects of drought on plant growth and photosynthetic physiology. *Oecologia* **2024**, *205*, 69–80. [CrossRef]
26. Liu, W.; Behzad, H.M.; Luo, Z.; Huang, L.; Nie, Y.; Chen, H. Species-specific root distribution and leaf iso/anisohydric tendencies shape transpiration patterns across heterogeneous karst habitats. *Plant Cell Environ.* **2025**, *48*, 199–212. [CrossRef]
27. Yan, Y.-M.; Fan, Z.-X.; Fu, P.-L.; Zhang, Z.-Y. Drought tolerance traits explain differential stem growth rates of evergreen and deciduous trees in a tropical karst forest. *Plant Divers.* **2025**, *47*, 454–465. [CrossRef]
28. Serrano-Finetti, E.; Castillo, E.; Alejos, S.; León Hilario, L.M. Toward noninvasive monitoring of plant leaf water content by electrical impedance spectroscopy. *Comput. Electron. Agric.* **2023**, *210*, 107907. [CrossRef]
29. Zhang, C.; Wu, Y.; Su, Y.; Xing, D.; Dai, Y.; Wu, Y.; Fang, L. A plant's electrical parameters indicate its physiological state: A study of intracellular water metabolism. *Plants* **2020**, *9*, 1256. [CrossRef]
30. Parkash, V.; Snider, J.L.; Virk, G.; Dhillon, K.K.; Lee, J.M. Diffusional and biochemical limitations to photosynthesis under water deficit for field-grown cotton. *Physiol. Plant.* **2024**, *176*, e14281. [CrossRef]
31. Xing, D.; Zhang, Q.; Wu, Y.; Zhao, K.; Wang, J.; Yan, S.; Li, Z. Use of transpiration water and leaf intracellular retained water in tomato (*Solanum lycopersicum* L.) plants subjected to different water supply strategies. *Sci. Hortic.* **2024**, *337*, 113520. [CrossRef]
32. Quispe-Puma, M.R.; Xing, D.; Wu, Y.; Zhang, Q.; Wang, J. Dynamic characteristics of leaf intracellular water, nutrients, metabolic energy, and photosynthetic responses to drought stress in maize. *Chil. J. Agric. Res.* **2025**, *85*, 677–688. [CrossRef]
33. Wei, P.; Li, H.; Wu, Y.; Zhang, C. Association of the electrical parameters and photosynthetic characteristics of the tea tree manifests its response to simulated karst drought. *Plant Signal. Behav.* **2024**, *19*, 2359258. [CrossRef]
34. Van Haeverbeke, M.; De Baets, B.; Stock, M. Plant impedance spectroscopy: A review of modeling approaches and applications. *Front. Plant Sci.* **2023**, *14*, 1187573. [CrossRef]
35. Xing, D.; Chen, X.; Wu, Y.; Li, Z.; Khan, S. Changes in elastic modulus, leaf tensity and leaf density during dehydration of detached leaves in two plant species of Moraceae. *Chil. J. Agric. Res.* **2021**, *81*, 434–447. [CrossRef]
36. Bartlett, M.K.; Klein, T.; Jansen, S.; Choat, B.; Sack, L. The correlations and sequence of plant stomatal, hydraulic, and wilting responses to drought. *Proc. Natl. Acad. Sci. USA* **2016**, *113*, 13098–13103. [CrossRef]
37. Wu, Y.-Y.; Liu, C.-Q.; Li, P.-P.; Wang, J.-Z.; Xing, D.; Wang, B.-L. Photosynthetic characteristics involved in adaptability to Karst soil and alien invasion of paper mulberry (*Broussonetia papyrifera* (L.) Vent.) in comparison with mulberry (*Morus alba* L.). *Photosynthetica* **2009**, *47*, 155–160. [CrossRef]
38. Wang, X.; Ma, X.; Ma, R.; Wang, B.; Tan, F.; Zhang, Q. Complementary strategies of hydraulic variability and conservative stomatal regulation enable widespread distributions in a heterogeneous karst landscape. *Ecol. Evol.* **2025**, *15*, e72744. [CrossRef]
39. Kovács, F.; Odry, Á.; Vizvári, Z.; Kabalan, S.; Papdi, E.; Odry, P.; Juhos, K. A novel approach to water stress assessment in plants: New bioimpedance method with PSO-optimized Cole-Cole impedance modeling. *Comput. Electron. Agric.* **2025**, *234*, 110167. [CrossRef]

40. Funk, J.L.; Larson, J.E.; Blair, M.D.; Nguyen, M.A.; Rivera, B.J. Drought response in herbaceous plants: A test of the integrated framework of plant form and function. *Funct. Ecol.* **2024**, *38*, 679–691. [CrossRef]
41. Yao, G.-Q.; Li, Y.-R.; Duan, Y.-N.; Han, S.-P.; Deng, Z.-J.; Yang, D.; Tian, X.-Q.; Li, F.-P.; Hasan, M.M.; Fang, X.-W. Stomatal and hydraulic redundancy allows woody species to adapt to arid environments. *Plant Cell Environ.* **2025**, *48*, 3406–3414. [CrossRef]

Disclaimer/Publisher's Note: The statements, opinions and data contained in all publications are solely those of the individual author(s) and contributor(s) and not of MDPI and/or the editor(s). MDPI and/or the editor(s) disclaim responsibility for any injury to people or property resulting from any ideas, methods, instructions or products referred to in the content.